Synthesis and Characterization of Ni/Mo Nanocatalysts on Alumina and Zeolite Supports

[1]**Olaremu** Abimbola G., [2]**Odebunmi** Ezekiel O. and [3]**Anderson** A. James

[1]Department of Chemical Sciences, Adekunle Ajasin University, Akungba Akoko, Nigeria.
[2]Department of Chemistry, University of Ilorin, Nigeria
[3]Surface Chemistry and Catalysis Group, Materials and Chemical Engineering, School of Engineering, University of Aberdeen, AB24 3UE, UK

Corresponding Author email address: abimbolaremu@yahoo.com / abimbola.olaremu@aaua.edu.ng

Abstract

A series of nickel/molybdenum bimetallic nanocatalysts were prepared by wet impregnation method on USY zeolite and alumina as support. The catalysts were characterized by nitrogen-sorption (for Brauneur-Emmet-Teller, BET surface area determination), X-ray diffractometry (XRD), Scanning Electron Microscopy (SEM), Scanning Electron Microscopy-Electron Dispersive X-ray Spectroscopy (SEM-EDX) , Transmission Electron Microscopy (TEM) and Temperature Programmed Reduction (TPR). The results of nitrogen sorption reveal a reduction of BET surface area of about 40% for nanocatalyst on alumina and zeolite. With the increase of zeolite content of our catalyst, the micropore volume and surface area increased while the average pore size decreased. Hence, as the micropores increased the mesopores and macropores decreased. The SEM surface morphologies of the catalysts confirmed that deposition of metals occurs in the pores and on the surface of the catalysts which have contributed to reduction in the surface area as indicated in the BET result. The EDX revealed the deposition of metals onto the surfaces. The presence of Al and Si in the support and Ni and Mo as active metals was confirmed. The TEM displayed a homogeneous dispersion of metals on the supports. The micrograph showed a worm-like motif with a random channel system which matches the plate-like particles assembled in parallel identified by the N_2-adsorption-desorption isotherm. However, the catalysts had darker coloration as the percentage of the zeolite was increased on the support due to the coating of pores with the metals which had better interactions as corroborated by the TPR profiles. The results of TPR showed that the weaker interaction between the Mo and Ni species and the support leads to better reducibility of the metal oxides on zeolite than on alumina. As the zeolite content of the mixed support was increased, the peak mainly due to the reduction of Mo became weaker, hence the reducibility of metal precursor on the support varies with different zeolite content.

Key words: Nanocatalysts; BET-Surface area; Temperature programmed reduction; Electron dispersive x-ray spectroscopy; Impregnation method

1. INTRODUCTION

The science of catalyst synthesis is a profitable venture. Market surveys in 2013 have shown the total sales of catalysts to be between $15 and$19 billion per year, and to increase by 4-5% per year (TMR, 2013; Freedonia Group, 2015). Most chemical processes, both established (Behrens *et al*., 2012; Babich and Moulijn, 2003; Brown et al., 2014) and emerging (Torre et al., 2012; Besson *et al.*, 2014; Huber *et al.*, 2006; Guo *et al.*, 2014) are performed using functional nanomaterials as catalysts. The field of catalyst synthesis, also known as catalyst preparation or catalyst manufacturing, is aimed at establishing the desired composition and structure of these materials (Munnik *et al.*, 2015). Over the years, different types and forms of cracking catalysts have been developed and used. The manner in which catalysts are built up from the separate components (catalyst assembly) and catalyst form have an important impact on their functionality (O'Connor *et al.*, 2001).

Alumina supported Mo(W)-sulfide catalysts with Nickel or Cobalt as promoters have long been used in the petroleum industries. The hydrocracking ability of the catalysts had been enhanced with more acid supports such as Zeolite and TiO_2 (Sayan and Paul, 2002; Furimsky, 2000; Ram *et al.*, 2005; Wang *et al.*, 2010; Arribas and Martiniz, 2002; Leite *et al.*, 2001; Hassan *et al.*, 2001). Apart from the conventional cracking function of the acidic sites, the catalytic activities and removal of heteroatoms are also improved with zeolite supports (Gallezot, 1979; Zheng *et al.*, 2008; Yasuda *et al.*, 1999).

Several studies dealt with SiO_2- supported Mo (Brito, 1986; Thomas *et al*., 1983; Shimada *et al.*, 1988; Biermann *et al.*, 1990; Henker *et al.*, 1991; Ismail *et al.*,1991; Lopez *et al.*, 1991) while a few dealt with SiO_2-Al_2O_3-supported systems (Brito, 1986; Thomas *et al*.,1983; Henker *et al*.,1991; Massoth *et al*., 1984; Henker *et al.*,1990; Rajagopal *et al.*, 1994). It is also generally accepted that molybdenum oxide on alumina support forms amorphous monolayers or 'Islands' on the alumina at Mo loading below 5 atom/nm^2 owing to the strong interaction with the support (Thomas *et al.*, 1982; Okamoto and Imanaka, 1988). The most active acidic carriers used in current hydrocracking catalyst are amorphous silica-alumina and zeolite (Scherzer and

Gruia, 1996). Zeolites based catalysts are more active and resistant towards deactivation by coke than those based on amorphous silica-alumina (Maxwell, 1987). Interestingly, zeolite catalysts are less selective towards the desired middle distillates as recracking of these products into lighter compounds increased by the presence of a large concentration of strong Bronsted acid sites associated with frame work alumina. Therefore, to improve the selectivity towards middle distillates, the zeolite-based catalysts can be modified to increase the framework silica-alumina ratio (Corma, 2004).

It has been reported that modifying the catalyst support leads to possible improvement of its activity, stability, and selectivity as the surface properties are manipulated (Biswas *et al.*, 2011). In this work, a series of Ni-Mo catalysts were prepared by the incipient wetness impregnation method. The metals were loaded on mixed support of γ-alumina and USY-zeolite in different proportions to give the final catalysts. The aim of this work is to investigate the effect of incorporation of catalysts on mixed supports on the reducibility, textural properties and particle size distribution.

2. EXPERIMENTAL PROCEDURE

Preparation of Ni-Mo/Alumina, Ni-Mo/Zeolite and Ni-Mo/Alumina-Zeolite catalysts

A nominal NiO loading of 3 wt % and MoO_3 loading of 14 wt % was chosen to have an atomic ratio of Ni/(Ni + Mo) close to 0.3. The catalysts were prepared via the wetness impregnation method. About 2.576 g of ammonium heptamolybdate tetra hydrate $(NH_4)_6Mo_7O_{24}.4H_2O$ was weighed and dissolved in 100 ml ultra-pure water (type 1), agitated for one hour and then impregnated with alumina supports. Afterwards, the mixture was dried overnight at 80°C. An aqueous solution of Ni using $Ni(NO_3)_2.6H_2O$ as the metal

Table 1: Composition of Ni-Mo Catalysts

Catalyst	Alumina (%)	USY Zeolite (%)
1. NiMo/Alumina	100	0
2. NiMo/Alumina (75 %)-Zeolite (25 %)	75	25
3. NiMo/Alumina (50 %)-Zeolite (50 %)	50	50
4. NiMo/Alumina(25 %)-Zeolite (75 %)	25	75
5. NiMo/Zeolite	0	100

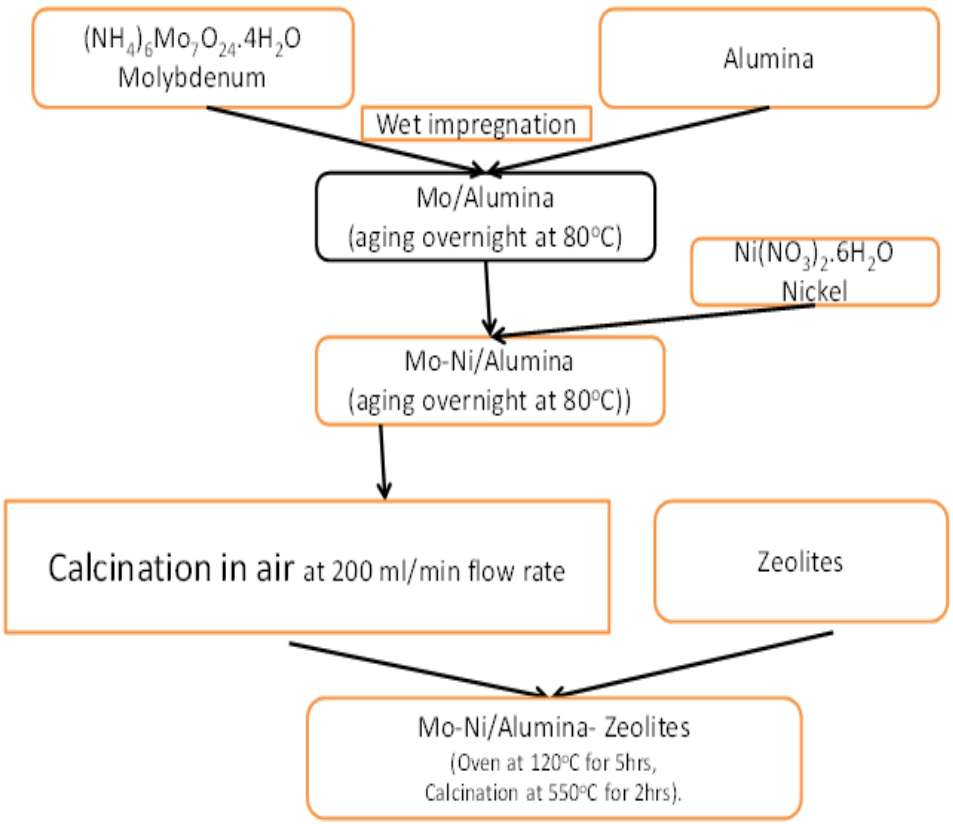

Figure 1: Synthesis of Ni-Mo/Alumina-Zeolite catalysts

precursor, was prepared by tailoring their concentration to the desired metal loading (1.486 g). The Mo-containing alumina material was impregnated with the corresponding Ni solution and dried overnight at 80°C. Finally, the material was calcined using the following temperature program: 150°C for 2 h, 350°C for 3 h, and finally 550°C for 4 h; the temperature rate employed was 10°C·min^{-1}. The calcination of the catalyst was carried out in a muffle furnace under flowing air at 200 mL·min^{-1}.

The procedure described above was followed for the preparation of Ni-Mo/Zeolite catalyst, except that USY zeolite was used as the support. The same procedure was adopted in the preparation of Ni-Mo/Alumina-Zeolite. The impregnated Mo-Ni/alumina powder was then mixed with USY zeolite according to the loading illustrated in Table 1, then deionised water was added to make a thick paste. The resulting solution was dried in an oven at 120°C for 5 hours and calcined at 550°C for 2 hours. Figure 1 presents the scheme used for the synthesis of Ni-Mo/Alumina-Zeolite catalysts.

3. CATALYSTS CHARACTERIZATION

Determination of Surface Area and Catalyst Particle Size by Nitrogen-adsorption/desorption

Brunauer-Emmett-Teller (BET) surface area, pore volume, and pore size measurements of the catalysts were performed using Micromeritics Tristar V4.02 analyser. Approximately 200 mg of each sample was degassed at 200°C for 2 hours under nitrogen flow to remove moisture prior to performing nitrogen adsorption tests based on the standard method of nitrogen adsorption at -196°C. The BET method was used to calculate the surface area and the pore size distribution was calculated with the BHJ method based on adsorption-desorption isotherms.

Determination of Catalyst Structure and Crystalline Properties by X-Ray Diffraction

Qualitative and quantitative determination of the nature of the phases and the amount of the phases present in the sample were determined by Panalytical X'Pert Pro diffractometer, employing Cu Kα monochromatic radiation. All the patterns were collected at room temperature with steps of 0.02˚ using a range of 5˚ - 80˚. The measurements were made at room temperature (298 K), with scan rate of 2˚ min^{-1} and 0.02 steps and the patterns were recorded by the Bruker-D8 softwareX-

Determination of Catalyst Morphology by Scanning Electron Microscopy

The morphology of each mesoporous support was examined by the Scanning Electron Microscopy (SEM) instrument. The SEM image of support sample was retrieved in a JEOL 840A SEM instrument. Powder samples were first spread on SEM slabs and sputtered with carbon

Determination of Elemental Composition by Scanning Electron Microscopy-Energy Dispersive X-Ray Analysis

The morphology and metal dispersion of the catalysts in oxide form was examined with a Hitachi S-3400 N SEM equipped with a Röntec XFlash of Si(Li) EDX analyser. Powder samples were first spread on SEM slabs and sputtered with gold. A qualitative elemental analysis was performed with EDX microanalysis at 2300x magnification.

Determination of Catalyst Structure by Transmission Electron Microscopy

Transmission Electron Microscopy was performed on the supports and the catalysts in oxide form. A JEOL 2011 Microscope equipped with a LaB6 gun and operating at 200 kV was used. The samples were finely grounded, suspended in ethanol and dispersed. A drop of this solution was then deposited on a classical TEM lacey carbon copper grid. TEM micrographs were taken focusing on parts of the samples lying across the grid holes to obtain information free of the contribution of the supporting carbon film.

Determination of Catalyst Reducibility by Temperature Programmed Reduction

The temperature programmed reduction (TPR) was carried out to investigate the reducibility of the oxide species of the calcined catalysts. In this experiment, two thermocouples were used; one was used for furnance control and one was placed in the well in the catalyst bed before entering the detector. Water and other condensable were frozen out of the gas in the cold tray, kept at 195 K. A carefully weighed 0.1 g of the sample was placed in quarts reactor between quartz wool plugs and loaded into the instrument. The experiments were performed at a heating rate of 10 °C min^{-1} from 40°C to 900°C with 5 % H_2 in nitrogen at 20 ml/min. The hydrogen consumption was measured by a thermal conductivity detector (TCD) attached to a TPDRO 1100 ThermoQuest CE instrument. The results generated were analysted by a Thermo Finnigan version 2.0 release 0.1 software that gives the results in TCD signal (mv), oven temperature versus temperature(s). The result was copied and analysed further with the aid of ORIGIN 7.0 analysis software.

4. RESULTS AND DISCUSSION

Nitrogen Gas Adsorption-Desorption and BET Surface Area Determination

The isotherms of the catalysts are presented in Figure 2 and Table 2 presents the textural properties of the catalysts determined by nitrogen-adsorption-desorption studies. According to Figure 2, all the catalysts exhibited Type IV physical adsorption isotherm at high relative pressure (p/p°) with hysteresis loops H_3 which corre-

Table 2: Textural Properties Of Catalysts Determined By Nitrogen Gas Absorption-Desorption Studies

Catalyst	BET Surface area (m^2/g)	Pore size (nm)	Micropore Volume (cm^3/g)
NiMo/Alumina	68.02	26.22	0.0031
NiMo/ Alumina (75 %)-Zeolite (25 %)	179.50	21.46	0.0513
NiMo/Alumina (50 %)-Zeolite (50 %)	214.61	19.43	0.0678
NiMo/ Alumina (25 %)-Zeolite (75 %)	398.18	13.17	0.1485
NiMo/Zeolite	434.94	10.31	0.1640

Surface area of Gamma Alumina used: 98 m^2/g, Surface area of Zeolite (H-SDUSY) CBV 901 used: 700 m^2/g

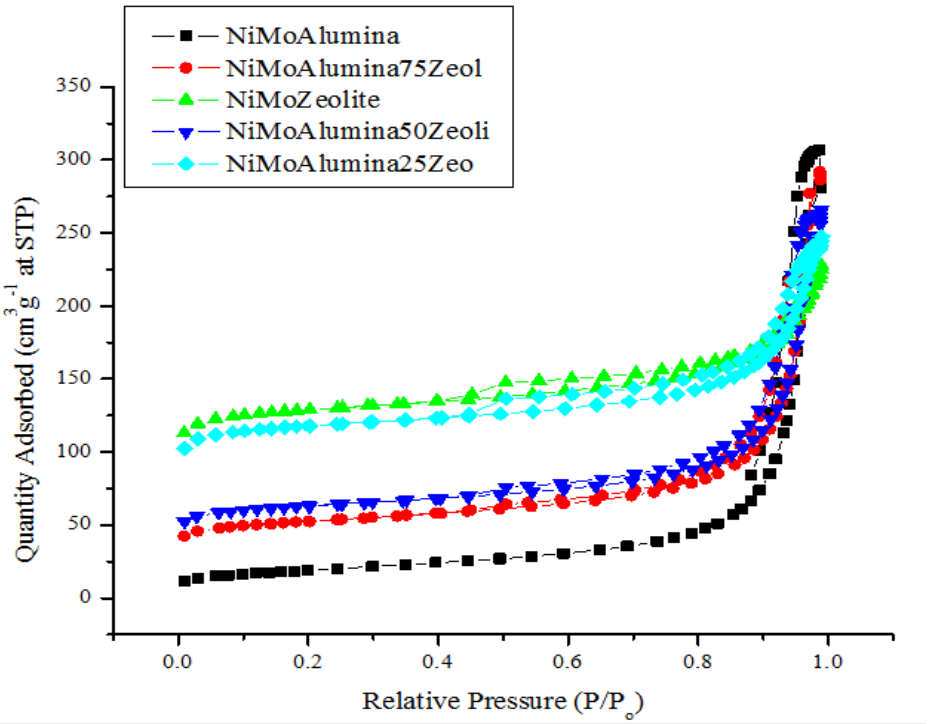

Figure 2: Nitrogen gas adsorptiondesorption isotherms of catalysts at different loading of Alumina and USY Zeolite

spond to materials with plate like particles and slit shaped pores (Sing *et al.*, 1985; Garg *et al.*, 2008; Gutiérrez *et al*., 2006; Kruk and Cao, 2007; Tanev and Pinnavaia, 1996). It was observed that NiMo/Zeolite presented lower average pore diameter (pore size) and higher surface area (S_{BET}) of the group with the highest pores.

It was observed that all materials presented a pore size in the mesoporous range. The hysteresis loop H_3 is representative of slit like platelets. Narrow hysteresis loops were observed for all synthesized catalysts. The nitrogen gas uptake capacity for the materials was similar at p/p^o values close to 1. The micro porosity of the materials was observed at low relative pressure of the isotherms. At high p/p^o values the curve for all of the synthesized catalysts continued upwards which is indicative of macro porosity (Sing *et al.*, 1985).

BET specific surface area, total pore volumes and average pore diameter of the synthesized catalysts are presented in Table 2. The N_2 adsorption–desorption isotherms of the supports and catalysts indicated that the support preserved its mesoporous structure after calcination and impregnation with metals.

There was a significant decrease in BET surface area and pore volume for alumina and zeolite after metal impregnation. Pore sizes of these catalyst samples were found to be less than those of the support (Alumina and USY-zeolite). The decrease in BET specific surface area and pore diameter after the impregnation of metal on the support indicated that metal nanoparticles were mainly incorporated inside the pore rather than on the surface of supports. The result is similar to what was reported by Sardar *et al.*, (2011) where a reduction of 40.5 % was recorded for bimetallic nanocatalysts on alumina. With the increase of zeolite content of our synthesized catalyst, the micropore volume and surface area increased, while the average pore size decreased. It has also been recently reported that as zeolite content increased, the micropores

of the catalysts increased, while the mesopores and macropores decreased (Zhang *et al.*, 2013). Hence, this is expected to enhance the hydrocracking ability of the catalysts. Besides the conventional cracking function of the acidic sites, the catalytic activities for hydrogenation of unsaturated compounds and removal of heteroatoms are also expected to improve with the zeolite supports (Gallezot, 1979; Zheng *et al.*, 2008 and Yasudu *et al.*, 1999).

X-ray Diffraction (XRD) Analysis

Figure 3 presents the X-ray diffraction patterns of USY zeolite and synthesized catalysts. For NiMo/ Alumina, three broad intensity peaks characterized the sample which matches the diffractogram reported in literature (Lesaint *et al.*, 2008). These peaks are typically assigned to gamma alumina suggesting some degree of ordering. All the catalyst diffractograms show no Ni or Mo oxide crystallite reflections; their diffraction patterns correspond to the one for alumina and zeolites respectively. This can suggest that Nickel and Molybdenum oxides were highly dispersed in the supports with a size of less than 4 nm, the detection limit of XRD technique (Maity *et al.*, 2005; Kaluza *et al.*, 2002; Dhar *et al.*, 2003; and Kim *et al.*, 2004)

The XRD patterns of all the other catalysts exhibited only broad XRD peaks of γ-alumina and zeolite even though the strength were reduced sharply, while no additional peaks belonging to crystalline Ni and Mo compounds were observed. The characteristic diffraction peaks of γ-Al_2O_3 and zeolite Y (2θ = 12°, 16°, 19°, 20° and 24°) appeared in all catalysts. The zeolite in Ni-Mo/Alumina-zeolite had a higher crystallinity than that in Ni-Mo/Alumina mainly due to the higher crystallinity of zeolite compared to alumina.

No detectable XRD crystalline forms of any Mo or Ni species were present in the oxidic catalysts, suggesting that the molybdenum and nickel oxidic species were either completely amorphous or composed of crystallites smaller than 4 nm. The peaks of zeolite in the small angle zone were more obvious with the increase of zeolite content in the mixed supports, a fact corroborated by Zhang *et al*., (2013).

Surface Morphology

Morphology plays an important role in activity and selectivity of catalyst. This can be observed by SEM analysis of the synthesized catalysts. Figure 4, shows high (10,000x) magnification SEM micrographs for the five catalysts.

The surface morphologies of the catalysts revealed a visible coating of metals blocking the pores observed in the catalysts. This is consistent with the observation

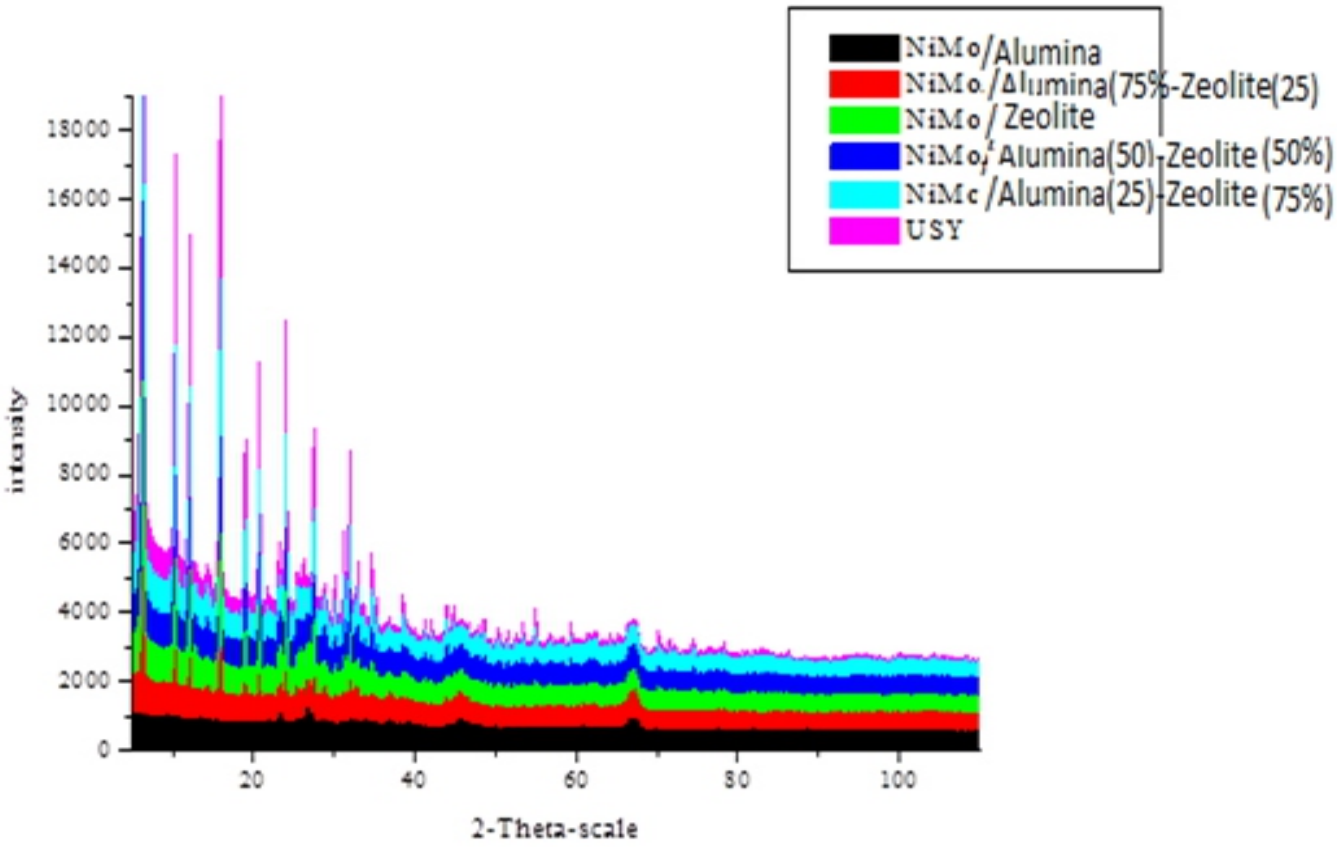

Figure 3: XRD patterns of zeolite (USY) and catalysts at different loading of alumina and USY Zeolite

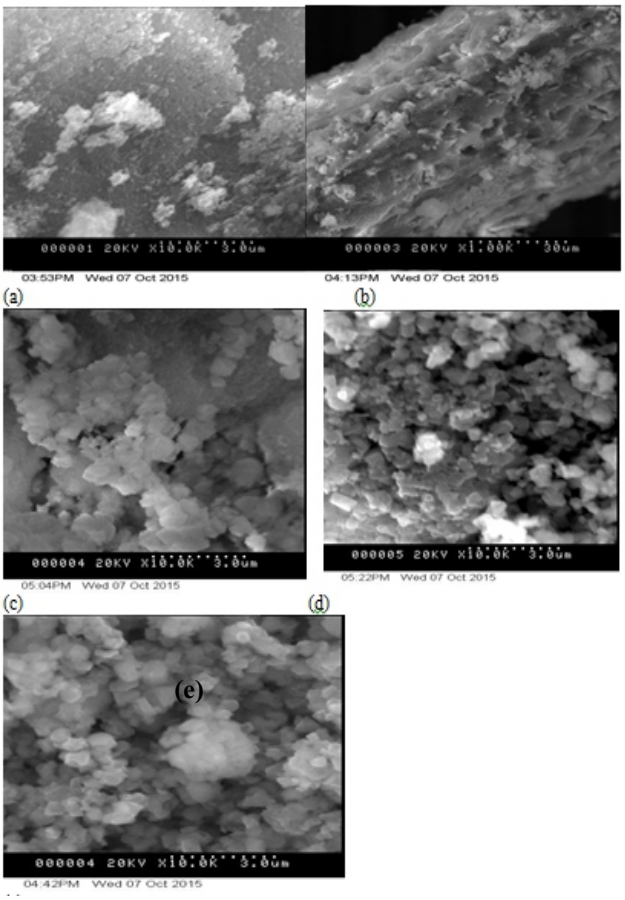

Figure 4: SEM micrographs of
(a) Ni-Mo/Alumina,
(b) Ni-Mo/Alumina (75 %)-Zeolite (25 %),
(c) Ni-Mo/Alumina(50%)-Zeolite(50%),
(d) Ni-Mo/Alumina(25%)-Zeolite (75%) and
(e) Ni-Mo/Zeolite at 10000X magnification**.**

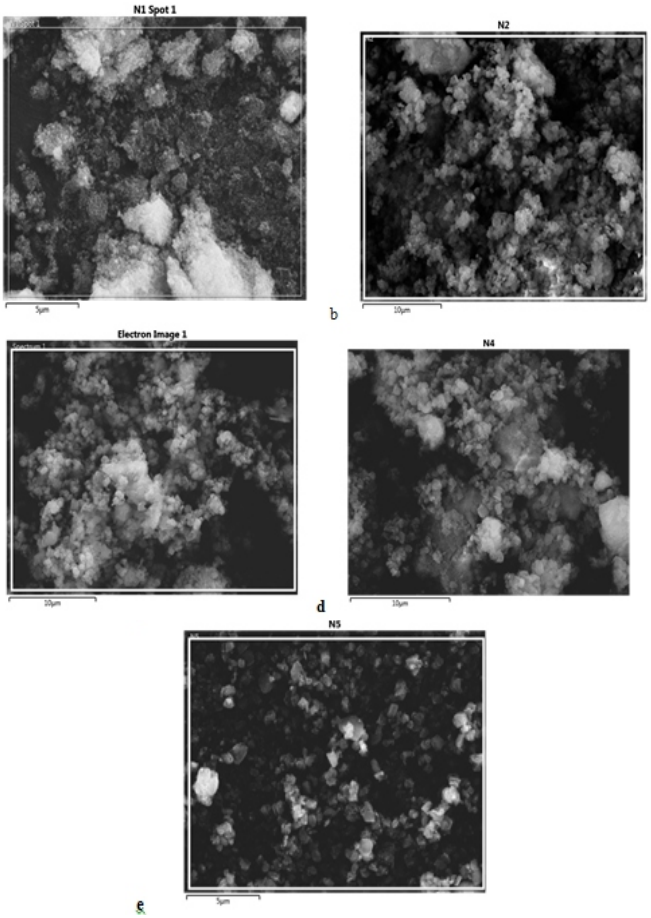

Figure 5: SEM micrographs of
(a) Ni-Mo/Alumina,
(b) Ni-Mo/Alumina (75 %)-Zeolite (25 %),
(c)Ni-Mo/Alumina (50%)-Zeolite(50%),
(d)Ni-Mo/Alumina (25%)-Zeolite(75%)
(e)Ni-Mo/Zeolite at 50000X magnification

in the nitrogen-adsorption-desorption studies. The decrease in the surface area was due to the incorporation of the metals into the pore of the supports. The SEM data provide detailed morphology with magnification up to 10000x allowing submicron-scale features such as metals which could not be observed with the XRD to be seen. It is clear that the deposition of metals occurs in the pores and on the surface of the catalysts which have contributed to reduction in the surface area. From the figures, the clusters are distributed around the catalyst surface and pore (Hart, 2014). From Figures 4 and 5, it can be seen that both magnifications of 10000X and 50000X, the five catalysts prepared have the morphology which tend to be agglomerate. From those figures, it can be seen that either there were small particles or large ones. It can also be observed that the catalyst morphology is arranged from flake-shaped box particles which formed an aggregate from small particles. It can be confirmed that the resulting catalysts still do not have a uniform size.

Elemental Composition of the Catalysts

The SEM-EDX analysis was used to study the surface morphology as well as to determine their elemental composition. The EDX mapped a small micro-area of the catalyst as presented in Figures 5 (a) to (e). The aim of the EDX was to confirm the presence of the species we incorporated. The analyzed results revealed the deposition of metals onto the surface of the catalyst. The presence of the elements in the support (Al, Si) and active metals (Ni, Mo) were confirmed. Cu was also detected as this element was present in the grid used to support the samples for analysis. The carbon was as a result of carbon coating before the catalysts were analyzed.

Microstructure of the Layered Catalysts

The representative TEM images of the catalysts are shown in Figures 6 to 8. The mesoporous structure of the different supports can be observed in the TEM micrographs at magnifications of 60,000, 150,000 and 600,000 for each material. The TEM images reveal the presence of typical layered structures. In order to find

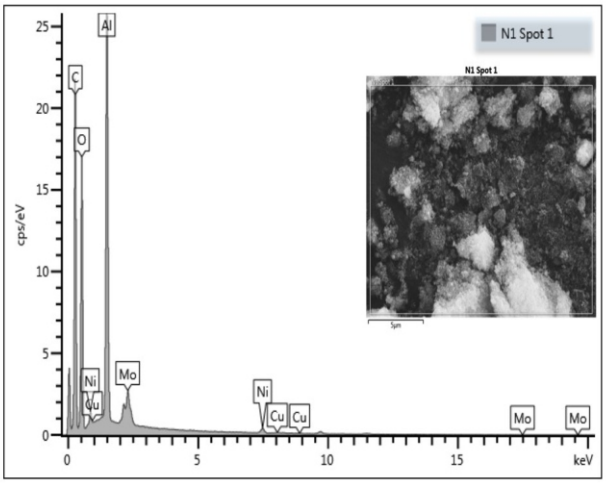

Figure 5(a): EDX analysis on SEM micrograph areas at 50,000x magnification (insert) for Ni-Mo/Alumina

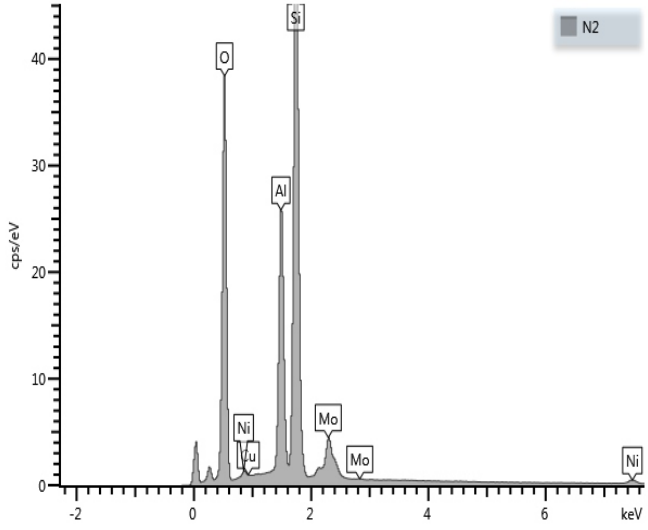

Figure 5(b): EDX for Ni-Mo/Alumina (75 %)-Zeolite (25 %)

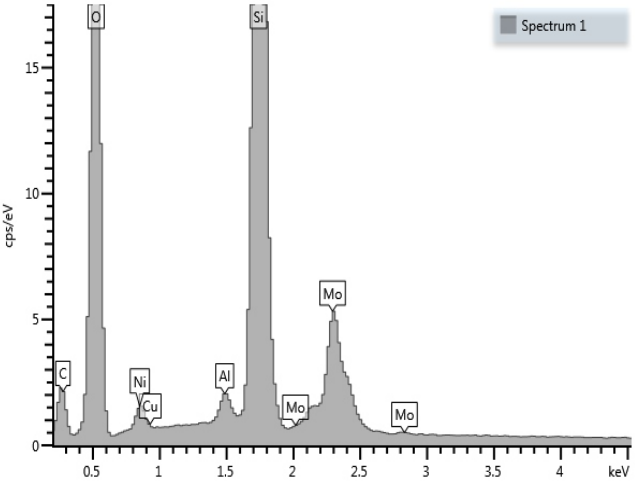

Figure 5(c): EDX for Ni-Mo/Alumina (50 %)-Zeolite (50 %)

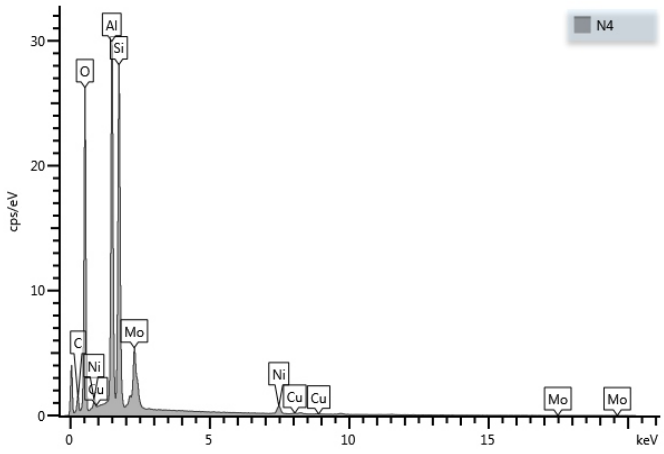

Figure 5(d): EDX for Ni-Mo/Alumina (25 %)-Zeolite (75 %)

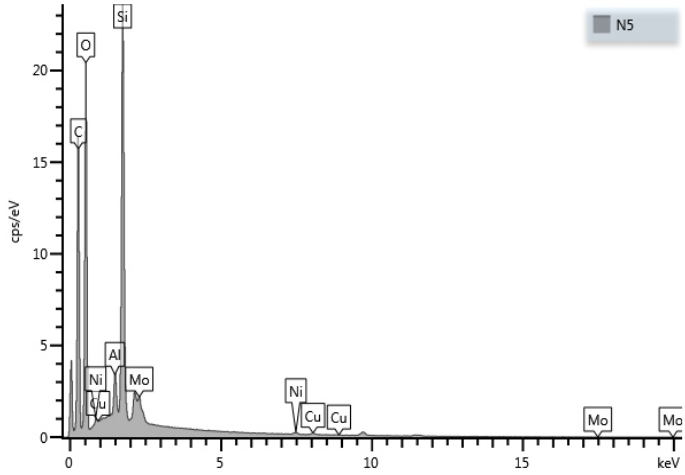

Figure 5(e): EDX for Ni-Mo/Zeolite

out the species and composition of the layered structure showing in TEM images, EDX analysis was carried out on several selected layered areas. EDX results showed that the species of the layered structure were composed of nickel and molybdenum. Therefore, the layered structure was demonstrated to be Ni-Mo. The intense peaks for each catalyst and constituents of the base materials are clearly stated.

The micrographs showed a worm-like motif with a random channel system representative of alumina (Zhang and Pinnavaia, 2002) which would match the plate-like particular in parallel identified by the N_2 adsorption-desorption. In the high magnification micrographs for all our materials, short corrugated platelets were detected as has been reported in literature (Lesaint *et al.*, 2008, González-Peña *et al.*, 2001))

A homogeneous dispersion for metals was observed for all the prepared catalysts. The catalysts had a darker coloration as the percentage/amount of zeolite was increased due to the coating of pores with molybdenum and nickel oxides which had better interactions as corroborated by the TPR profiles.

It is obvious that the metals are well dispersed on the supports forming a worm-like motif. TEM micrographs in Figure 6– 8, revealed the micro-images of Ni-

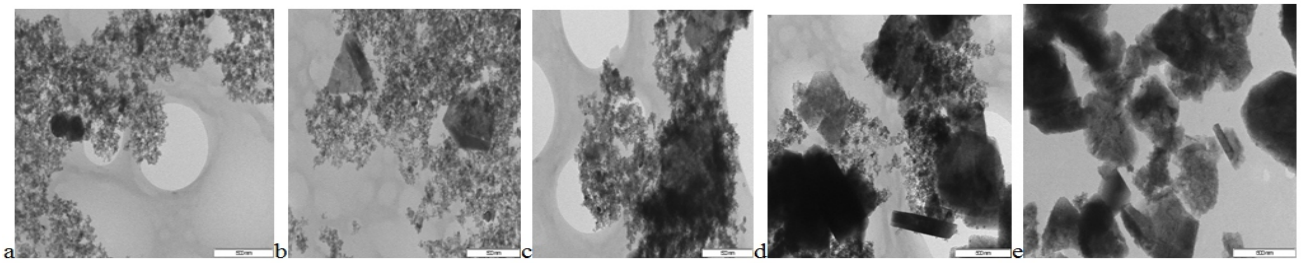

Figure 6: TEM micrographs of (a) Ni-Mo/Alumina, (b) Ni-Mo/Alumina (75 %)-Zeolite (25 %), (c) Ni-Mo/Alumina (50%)-Zeolite(50%), (d) Ni-Mo/Alumina (25%)-Zeolite (75%) and (e) Ni-Mo/Zeolite at 60,000 magnification

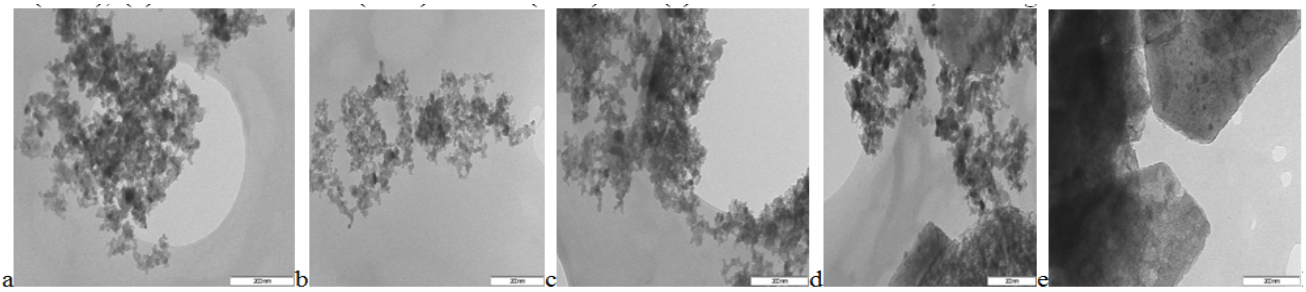

Figure 7: TEM micrographs of (a) Ni-Mo/Alumina, (b) Ni-Mo/Alumina (75 %)-Zeolite (25 %), (c) Ni-Mo/Alumina (50%)-Zeolite(50%), (d) Ni-Mo/Alumina (25%)-Zeolite (75%) and (e) Ni-Mo/Zeolite at 150,000 magnification

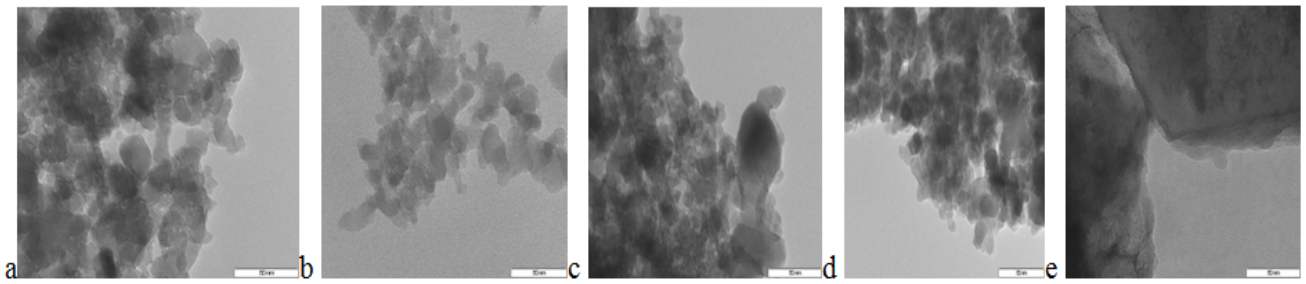

Figure 8: TEM Micrographs of (a) Ni-Mo/Alumina, (b) Ni-Mo/Alumina (75 %)-Zeolite (25 %), (c) Ni-Mo/Alumina (50%)-Zeolite(50%), (d) Ni-Mo/Alumina (25%)-Zeolite (75%) and (e) Ni-Mo/Zeolite at 600,000 magnification

Mo on alumina and zeolite supports at different magnifications. The composition of the supports was varied and had impact on the interaction between the metal and the supports. There was homogeneous dispersion of metals on the supports but from the micrograph, the catalysts had darker coloration as the percentage of the zeolite was increased on the support due to the coating of pores with the metals.

Hydrogen Reduction

The reducibility of the prepared catalysts was studied by H_2-temperature-programmed reduction (TPR). Figure 9 shows the results of TPR experiments of the catalysts and the peak positions summarized in Table 3. Three main peaks were observed for all the supported catalysts where a low temperature Mo reduction first appears, followed by the Ni reduction and then a high temperature Mo reduction. The first molybdenum peak corresponds to a reduction of octahedral Mo. ($Mo^{6+} \rightarrow Mo^{4+}$) and the second to a reduction of tetrahedral species ($Mo^{4+} \rightarrow Mo$) (Lopez *et al.*, 1991; Qu *et al.*, 2003; Alibouri *et al.,* 2009). Nickel species are reduced in a single step (Li and Chen, 1995).

Reduction of nickel supported catalyst is difficult (Chen and Shiue, 1988) and the equilibrium between oxidic Ni and H_2 varies depending on the extent of interaction between Ni and the support. The interactions between Ni and the support can be characterized by the reducibility of nickel. Some studies have shown that nickel supported on alumina is not completely reduced to the metallic state due to a strong oxide support interaction (Chem and Shiue, 1988; Martin *et al.*, 1973). However, the reduction depends on metal loading and calcination temperature and has been attributed to the formation of nickel aluminate spine (Shalvoy and Reucroft, 1977) or to nickel ions in the tetrahedral and octahedral sites of alumina (Wu and Hercules, 1979), or to a modification of the electronic properties of nickel oxide due to reduction with alumina (Hollinger *et al.*, 1978). Li and Chen, (1995) investigated two series of NiO/Al_2O_3 catalysts with various metal loadings prepared by incipient-wetness impregnation and co-precipitation methods. The reducibility of NiO over these catalysts was

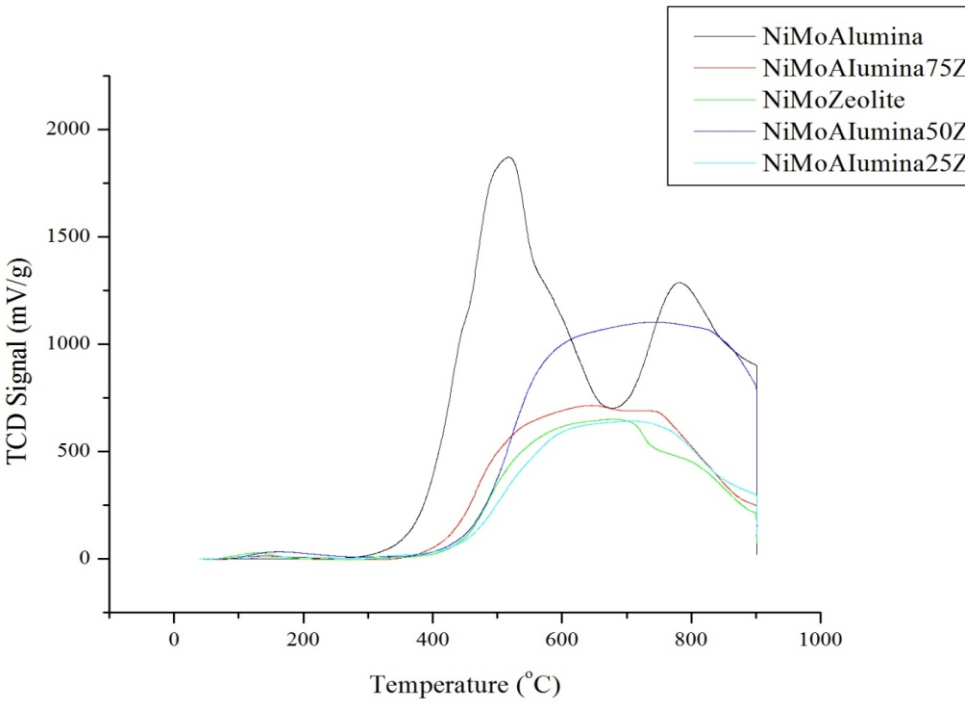

Figure 9: TPR Profile of different catalysts

Table 3: Hydrogen- TPR Data for the Catalysts

Catalyst	Reduction temperature (°C)		
	Peak 1	Peak 2	Peak 3
NiMo/Alumina	517	563	781
NiMo/Alumina (75 %)-Zeolite (25 %)	141	647	740
NiMo/Alumina (50 %)-Zeolite (50 %)	148	744	822
NiMo/Alumina (25 %)-Zeolite (75 %)	144	709	748
NiMo/Zeolite	126	677	790

investigated by the temperature programmed reduction technique. For impregnated Ni/Al_2O_3 catalysts, more than one species was detected by TPR. At low nickel loadings NiO was observed. The rate of reduction of NiO on support depends not only on the chemical nature of the NiO species but also on the rate of nucleation of metallic nickel. At high nickel loadings due to the presence of easily reduced Ni species, the rate of reduction is enhanced.

Jerzy (1982) also reported that the TPR curve for pure nickel oxide powder had a single peak of hydrogen consumption with a maximum at 230°C. For the supported catalysts of high nickel concentration two hydrogen consumption peaks appear on the TPR curves. The first, low temperature peak appeared at much the same temperature as for pure nickel oxide; the other, very broad has a maximum at 450°C. For supported catalysts of low nickel concentration only the high temperature peak of hydrogen consumption was observed.

Qu *et al.*, (2003) evaluated the interaction between Ni and Mo species and catalysts containing only Ni or Mo and both under the applied conditions, all the species were reduced. For Ni/Al_2O_3, the reduction temperature was a broad band centered between 640 and 800°C which is a higher temperature than for bulk NiO with a single reduction peak at around 300°C (Briton and Laine, 1986). Mo/Al_2O_3 showed two main peaks one at 422°C and the other at 874°C, with a shoulder observed at 710°C which may be due to the intermediate- reducible crystalline phases of orthorhombic MoO_3 and $Al_2(MoO_4)_3$ (Rajagopal *et al.*, 1994; Arnoldy *et al.*, 1985; Brito et al., 1989; and Marzari *et al.*, 1995). With the incorporation/addition of Ni into Mo/Al_2O_3, the TPR profile shifted to lower temperature. Peaks appeared at 370, 593 and 830°C. After the Ni content and calcination temperature of the NiMo supported on alumina was changed, the peak that appeared at 590°C was assigned to the reduction of Ni species (Brito and Laine, 1986). The peaks for the Mo species changed from 422°C to 370°C and 874°C to 830°C which indicated a shift of about 40 to 50 to a lower temperature, indicating that the addition of Ni promoted the reducibility of Mo. The reduction of Ni

species was also promoted showing a maximum at 593°C. Our results (Table 3) was supported by Breysse *et al.*, 1997; Simon *et al.*, (2001) and Inamura *et al.*, (2011) who also observed the different reducibility of the metal precursor on the supports with different zeolite contents.

5. CONCLUSION

The SEM, TEM and SEM-EDX analysis showed that the catalysts were crystalline and EDX data confirmed the presence of Al and Si in the support and Ni and Mo as active metals. We can conclude that the results of temperature programmed reduction showed the weak interaction between the Mo and Ni species and the support leads to better reducibility of the metal oxides on zeolite than on pure alumina. There are also larger pores on the zeolite support than on the alumina support which will result in higher hydrocracking activity of Ni-Mo catalysts supported on zeolite. It was observed that with the increase of zeolite content, the peak mainly due to the reduction of Mo species, became weaker, which indicates that metal oxides on the catalyst surface was more difficult to be reduced since the metal support interaction was modified with the addition of Zeolite. Finally, the interaction between active phase precursor and the support, the acidity change the electronic properties of the metal and therefore modify the properties of the catalysts.

ACKNOWLEDGMENT

The authors are grateful to Tertiary Education Trust Fund (TETFUND) and Adekunle Ajasin University Akungba Akoko for supporting the postgraduate studies of Dr. Olaremu, A.G. We also wish to appreciate members of Surface Chemistry and Catalysis Group, School of Engineering, University of Aberdeen, and the University of Aberdeen for admitting him as a visiting researcher to the institution.

REFERENCES

Alibouri, M., Ghoreishi, S.M. and Aghabozorg, H.R. (2009) "Hydrodesulfurization Activity of NiMo/Al-HMS Nanocatalyst Synthesized by Supercritical Impregnation".Industrial and Engineering Chemistry Research. 48(9):428392.

Arnoldy, P., de Jonge, J.C.M and Moulijn, J.A (1985) "Temperature programmed reduction of molybdenum (VI) oxide and (IV) oxide". Journal of Physical Chem, 89:4517.

Arribas M A. and Martinez A. (2002). "The influence of zeolite acidity for the coupled hydrogenation and ring opening of 1−methylnaphthalene on Pt /USY catalysts" J. Appl Catal A: Gen, 2002, 230(1/ 2):203−217.

Babich, I.V. and Moulijn, J.A. (2003) "Science and technology of novel processes for deep desulfurization oil refinery streams : A review". Fuel. 82:607 631.

Behrens, M.; Studt, F.; Kasatkin, I.; Kühl, S.; Hävecker, M.; Abild- Pedersen, F.; Zander, S.; Girgsdies, F.; Kurr, P.; Kniep, B.-L.; Tovar, M.; Fischer, R.W.; Nørskov, J.K.; Schlögl and R. (2012). "The active site of methanol synthesis over $Cu/ZnO/Al_2O_3$ industrial catalysts." Science. 336:893-897.

Besson, M.; Gallezot, P. and Pinel, C. (2014). "Conversion of biomass into chemicals over metal catalysts". Chem. Rev. 114(3):1827-70.

Biermann, J.J.P., F.J.J.G. Janssen, M. de Boer, A.J. van Dillen, J.W. Geus, and E.T.C. Vogt, (1990). "Molybdena on silica catalysts: selective catalytic oxidation of ammonia to nitrogen over MoO_3 on SiO_3 catalyst" . J. Mol. Catal. 60 (2):229-238.

Biswas, P., Narayanasarma, P., Kotikalapudi, M.C., Ajay, K.D. and John, A. (2011). "Characterization and activity of ZrO_2 doped SBA-15 supported NiMo catalysts for HDS and HDN of bitumen derived heavy gas oil", Ind. Eng. Chem. Res., 50:7882-7895.

Breysse, M., Cattenot, M., Kougionas, V., Lavalley, J.C., Mauge, F., Portefaix, J.L. and Zotin, J.L. (1997). "Hydrogenation properties of ruthenium sulfide clusters in acidic zeolite" Journal of Catalysis 168(2):143-153.

Brito, J., Laine, J and Pratt, K.C. (1989) "Temperature programmed reduction of Ni-Mo Oxide." Journal of Material Science 241:245.

Brito, J. and Laine, (1986). "Characterization of supported MoO_3 by temperature-programmed reduction" J. Polyhedron 5 (1/2):179-182.

Brown, D.E.; Edmonds, T.; Joyner, R.W.; McCarroll, J.J. and Tennison, S.R. (2014). "The genesis and development of the commercial BP doubly promoted catalyst for ammonia synthesis" Catal. Lett. 144:545-552.

Chen, I. and Shiue, D.W. (1988) "Reduction of nickel-alumina catalysts" lnd. Eng. Chem. Res., 27,429-434.

Corma, A., Diaz-Cabanas, M.J., Lopez, C. and Martinez, A. (2004). "Hydrocracking Catalysts based on the new large-pore ITQ-21 Zeolite for maximizing Diesel Products". Studies in Surface Science and Catalysis, 154:2380-2386.

Dhar, G.M., Srinivas, B., Rana, M., Kumar, M. and Maity S. (2003) "Mixed oxide supported hydrodesulfurization catalystsa review". Catalysis Today; 86(14):4560.

Freedonia Group. World Catalysts, 2013. www.freedoniagroup. com/world-catalysts.html (accessed on January 2, 2015).

Furimsky E .(2000). "Catalytic hydrodeoxygenation" J. Appl Catal A: Gen, 199(2):147−190.

Gallezot P. (1979). "The state and catalytic properties of platinum and palladium in faujasite−type zeolites". Cat Re−Sci Eng, 20(1): 121− 154.

Gallezot P. (1979). "The state and catalytic properties of platinum and palladium in faujasite−type zeolites" J. Cat Re−Sci Eng, 20(1):121−154.

Garg, S., K. Soni, G.M. Kumaran, M. Kumar, J.K. Gupta, L.D. Sharma and G.M. Dhar (2008) "Effect of Zr-SBA-15 support on catalytic functionalities of Mo, CoMo, NiMo hydrotreating catalysts," Catalysis Today. 130:302-308.

global-refinery-catalyst-market.html (accessed on January 2, 2015).

González-Peña V, Díaz I, Márquez-Alvarez C, Sastre E, Pérez-Pariente J. (2001) "Thermally stable mesoporous alumina synthesized with non-ionic surfactants in the presence of amines". Microporous and Mesoporous Materials; 44-45:20310.

Guo, X.; Fang, G.; Li, G.; Ma, H.; Fan, H.; Yu, L.; Ma, C.; Wu, X.; Deng, D.; Wei, M.; Tan, D.; Si, R.; Zhang, S.; Li, J.; Sun, L.; Tang, Z.; Pan, X. and Bao, X. (2014). "Direct, non oxdidative conversion of methane to ethylene, aromatics and hydrogen". Science, 344:616-619.

Gutiérrez, O.Y., Fuentes, G.A., Salcedo, C. and Klimova, T. (2006). "SBA-15 supports modified by Ti and Zr grafting for NiMo hydrodesulfurization catalysts." Catalysis Today.

116:485-497.
Hart Abarasi (2014). "Advanced Studies of Catalytic Upgrading of Heavy Oils" Ph.D. Thesis. School of Chemical Engineering. University of Birmingham, UK.
Hassan A, Ahmed S, Ali M.A, Hamid H and Inui T.A.(2001). "Comparison between [beta]−and USY−zeolite−based hydrocracking catalysts." J. Appl. Catal. A: Gen, 220(1/2):59−68.
Henker, M,. K.-P. Wendlandt, E.S. Spiro and O.P. Tkachenko (1990), "Phase and surface composition and dispersion of MoO_3 in MoO_3/Al_2O_3-SiO_2 catalysts" Appl. Catal. 61:253-263.
Henker,M,. K.-P.Wendlandt, J. Valyon, P. Bornmann, (1991). "Structure of MoO_3/Al_2O_3-SiO_2 catalysts." Appl. Catal. 69:205-220.
Hollinger, G., Uc, T.M.D and Vedrine, J.C. (1978). "Investigations of antigerite and nickel supported catalysts by X-ray photoelectron spectroscopy" J. Phys. Chm, 82:1515.
Huber, G. W.; Iborra, S. and Corma, A. (2006). "Synthesis of transport fuels from biomass: chemistry, catalysts and engineering." Chem. Rev. 106:4044-4098.
Inamura, K. and Iino, A. (2011). "Development of zeolite hydro-cracking catalyst and system for resid hydrodesulfurization unit." J. Catal. 164(1):204-208.
Ismail, H.M. M.I. Zaki, G.C. Bond, and R. Shukri, (1991) "Temperature-programmed reduction of MoO_x/SiO_x and $MoOx/Al_2O_3$ catalysts and surface structural consequences of impregnation acidity" Appl. Catal. 72:L1-L12.
Jerzy Zielinski (1982). "Morphology of Nickel/ Alumina catalysts"; Journal of Catalysis 76:157-163.
Kaluza L., Zdrazil M., Zilková N. and Cejka J. (2002). " High activity of highly loaded MoS_2 hydrodesulfurization catalysts supported on organised mesoporous alumina". Catalysis Communications; 3(4):151157.
Kim, P., Kim, Y., Kim, H., Song, I.K. and Yi, J. (2004). "Synthesis and characterization of mesoporous alumina with nickel incorporated for use in the partial oxidation of methane into synthesis gas". Applied Catalysis A: General; 272(1-2):15766.
Kruk, M. and L. Cao, (2007). "Pore size tailoring in large-pore SBA-15 silica synthesized in the presence of hexane," Langmuir. 23:7247-7254.
Leite L, Benazzi E. andMarchaL−George N. (2001). Hydrocracking of phenanthrene over bifunctional Pt catalysts [J]. Catal. Today, 65 (2/4):241−247.
Lesaint C, Glomm WR, Borg Ø, Eri S, Rytter E. and Øye G. (2008) "Synthesis and characterization of mesoporous alumina with large pore size and their performance in Fischer-Tropsch synthesis". Applied Catalysis A: General. 351(1):131135.
Li C, Chen Y-W (1995). "Temperature-programmed-reduction studies of nickel oxide/alumina catalysts: effects of the preparation method". Thermochimica Acta., 256(2):45765.
López, Cordero R, Gil Llambias F.J, and López Agudo A. (1991). "Temperature-programmed reduction and zeta potential studies of the structure of $Mo/O_3Al_2O_3$ and Mo/O_3SiO_2 catalysts effect of the impregnation pH and molybdenum loading". Applied Catalysis; 74(1):12536.
Maity, S.K, Ancheyta, J. and Rana M.S. (2005). "Support Effects on Hydro processing of Maya Heavy Crude". Energy Fuels; 19(2):3437.
Martin, G.A., Ceaphalan, N. and Moutgolfier, P.D. (1973). " 2 states of chemisorptions of H_2 on supported nickel-catalyst, evidenced by measurements of saturation magnetization" J. Chem. Phys., 70:1422-1427.
Marzari, J.A., Rajagopal, S. and Miranda, R.J. (1995). "Bifunctional mechanism of pyridine hydrodenitrogenation." Catal. 156: 255.
Massoth, F.E, G. Muralidhar and J. Shabtai, (1984). "Catalytic functionalities of supported sulfides: II. Effect of support on Mo dispersion. J. Catal. 85:53-62.
Maxwell, I.E., (1987). "Zeolite catalysis in hydro processing." Catal. Today, 1:385-413.
O'Connor, P; Imhof, P. and Yanik, S.J. (2001). "Catalytic Assembly Technology in Fluid Catalytic Cracking V". Material and Technology Innovations, Studies in Surface Science and Catalysis, Occelli, M.L.; O'Connor, P. (Eds.), Vol. 134.
Okamoto,Y. and T. Imanaka, (1988). 'Interaction chemistry between molybdena and alumina: infra-red studies of surface hydroxyl groups and adsorbed carbon J. Phys. Chem. 92:7102.
Peter Munnik, Petra E. de Jongh, and Krijn P. de Jong (2015). "Recent Developments in the Synthesis of Supported Catalysts". Chem. Rev. 115:6687−6718.
Qu L, Zhang W, Kooyman P.J. and Prins R. (2003) "MAS NMR, TPR and TEM studies of the interaction of NiMo with alumina and silicaalumina supports". Journal of Catalysis. 215(1):713.
Rajagopal, S., Marini, H,J., Marzari, J. and Miranda, R. (1994). "Silica-Alumina-supported Acidic Molybdenum catalysts-TPR and XRD Characterization" .J. Catal 147(2):417-428.
Ram Rez J, Rayo P, Guti Rrez−Alejandre A, Ancheyta J and Rana M S. (2005). "Analysis of the hydrotreatment of Maya heavy crude with NiMo catalysts supported on TiO_2−Al_2O_3 binary oxides: Effect of the incorporation method of Ti." J. Catal. Today, 109(1/4):54−60.
Sardar, Ali., Noor Asmawati, Mohd Zabidi and Duvvuri Sabbarao (2011). "Synthesis and characterization of Co/Mo Bimetallic Nanocatalysts". Journal of Materials Science and Engineering A1:390-397.
Sayan S. and Paul J. (2002). "Hydrogenation of naphthalene and methylnaphthalene: modeling and spectroscopy" J. Mol Catal A: Chem, 185 (1/2):211−222.
Scherzer, J., and Gruia, A.J. (1996). "Hydrocracking Science and Technology", Marcel Dekker, New York. Chap. 12, p. 215.
Shalvoy, R.B and Reucroft, P.J. (1977). "Quantitative analysis of ESCA signal intensities from coprecipitated nickel on alumina catalysts". J. Electron Spectrosc. Relat. Pheman. 12:351-356
Shimada, H,. T. Sato, Y. Yoshimura, J. Hiraishi and A. Nishijima (1988). "Supported effect on the catalytic activity and properties of sulfide molybdenum catalysts" J. Catal. 110:275-284.
Simon, L.J., Van Ommeen, J.G., Jentys, A. and Lercher, J.A. (2001)." Sulfur-tolerant Pt-supported zeolite catalysts for benzene hydrogenation: Influence of the support." J. Catal, 201(1);60-69.
Sing K.S.W. Everett D.H., Haul R.A.W., Moscou L., Pierotti R.A. and Rouquerol J. (1985). "Reporting physisorption data for gas/solid systems". Pure Appl Chem. 57(4):60319.
Tanev, P.T and Pinnavaia, T.J (1996). "Mesoporous silica molecular sieves prepared by ionic and neutral surfactant templating: a comparison of physical properties "Chemistry of Materials 8:2068-2079.
Thomas, R,.E. M. van Oers, V.H.J. de Beer, J. Madema, J.A. Moulijn (1982). "Characterization of γ-alumina-supported molybdenum oxide and tungsten oxide; reducibility of the oxidic sulfide state versus hydrodesulfurization activity of the sulfide state". J. Catal. 76:241.

Thomas, R,. E.M. van Oers, V.H.J. de Beer and J.A. Moulijn, (1983). "Characterization of silica-supported molybdenum oxide and tungstem oxide. Reducibility of the oxidic state versus hydrosulfurization activity of the sulfide state." J. Catal. 84:275.

Torres Galvis, H.M.; Bitter, J.H.; Khare, C.B.; Ruitenbeek, M.; Dugulan, A.I. and de Jong, K.P. (2012). "Supported iron nanoparticles as catalysts for sustainable production of lower olefins". Science, 335:835-838.

Transparency Market Research. (2013). "Refinery (FCC, Hydrocracking, Catalytic Reforming), Synthesis, Polymer and Environmental Catalyst Market" Global Industry Analysis by Material (Zeolites, Metal, Others), by Type (Homogenous and Heterogeneous), Catalyst Regeneration (Off-Site and On-Site), Size, Share, Growth, Trends and Forecast 2012−2018. www.transparencymarket research.com/.

Trimm, D L and Stanislaus A. (1986). "The control of pore size in alumina catalyst supports": A review. Applied Catalysis ; 21(2):21538

Wang L, Shen B, Fang F, Wang F, Tian R, Zhang Z and Cui L. (2010). "Upgrading of light cycle oil via coupled hydrogenation and ring−opening over NiW/Al_2O_3−USY catalysts [J]." Catal Today, 2010, 158(3/ 4): 343−347.

Wu, M and Hercules, D.M (1979) "Studies of supported nickel catalysts by X-ray photoelectron and ion scattering spectroscopies" J. Phys. Chem, 83:2003.

Yasuda H, Sato T. and Yoshimura Y. (1999). "Influence of the acidity of USY zeolite on the sulfur tolerance of Pd−Pt catalysts for aromatic hydrogenation [J]." Catal. Today, 1999, 50(1):63−71.

Zhang Z, Pinnavaia T.J. (2002). "Mesostructured γ-Al_2O_3 with a Lathlike Framework Morphology." J. Am. Chem. Soc.; 124(41):12294301.

Zhang, Hai-yong., Wang, yong-gong., Zhang, Pei-Zhong., Lin, Xiong-Chao. and Zho, Yu Pei (2013). "Preparation of NiW catalysts with alumina and zeolite Y for hydrprocessing of coal tar". Journal of Fuel Chemistry and Technology 0253-2409: 09-1085-07.

Zheng, J., Guo, M. and Song, C. (2008). "Characterization of Pd catalysts supported on USY zeolites with different SiO_2/Al_2O_3 ratios for the hydrogenation of naphthalene in the presence of benzothiophene". Fuel Process Technol. 89(4):467−474.